Coupled Heat Transfer Characteristics of SiC High Temperature Heat Exchanger in Solid Oxide Fuel Cell

Jia-Liang Song[1](✉), Hua Chen[2], Yong-Dong Chen[1], Gai-Ge Yu[1], Hong-Wei Zou[1], and Bing-Chuan Han[1]

[1] Hefei General Machinery Research Institute Co., Ltd. (HGMRI), Hefei 230031, China
sjl516516@126.com, chenyongdong@hgmri.com
[2] University of Science and Technology of China, Hefei 230027, China

Abstract. High temperature heat exchanger is a crucial equipment in the BOP of SOFC. Replacing the commonly used metal materials with high-temperature resistant SiC ceramic materials for the manufacturing of SOFC high-temperature heat exchanger is a revolutionary technology with great application potential. This paper focused on SiC-based cathodic air preheater which is a novel SOFC high temperature heat exchanger, and firstly investigated the coupled radiation-conduction-convection heat transfer characteristics between flue gas and air at extremely high temperature conditions. The DO model in ANSYS Fluent was utilized to analyze the radiation heat transfer characteristics of high-temperature flue gas and the effect of gas absorption coefficient, and the simulation results were compared with the S2S model and non-radiation model. The results showed that radiation heat transfer cannot be ignored at high flue gas inlet temperature. With flue gas inlet temperature in the range of 800–1100 °C and low air/flue gas flow rate ratio, the gas radiation heat transfer and the effect of flue gas absorption coefficient can be ignored.

Keywords: SOFC · Cathode air preheater · SiC · Heat radiation · Coupled heat transfer characteristics

1 Introduction

In China, Solid oxide fuel cell (SOFC) is favorable in heat power cogeneration and is of great significance in supporting the "dual carbon" target [1]. At present, the fledgling SOFC industry in China mainly focused on the research of stack, however the focus on the BOP (Balance of Plant), which is another major component of SOFC, is not enough. BOP is the crucial technology in SOFC including functions of inlet/outlet gas heat exchange, fuel/air flow distribution, waste heat utilization and so on. It is the key to ensure the efficient and stable operation of the stack.

The operating temperature of SOFC is in the range of 700–1000 °C. It is required that the cathode inlet air temperature of the stack should not be less than 700 °C after stable operation. The BOP recovers the unreacted anode fuel and cathode air of the stack, and

H. Sun et al. (Eds.): WHTC 2023, SPPHY 393, pp. 200–213, 2024.
https://doi.org/10.1007/978-981-99-8631-6_23

sends them to the catalytic combustion chamber for full combustion. The combustion exhaust preheats the cathode air in the high temperature heat exchanger to an appropriate temperature range and then enters the stack to participate in the reaction.

For the high temperature heat exchanger, on the one hand, the increasing stack reaction temperature has the risk of exceeding the temperature tolerance limit of metal heat exchanger represented by superalloy materials. On the other hand, the long-term use of typical commercial metal alloy heat exchanger suffers from the risk of chromium volatilization, which is a known cathodic degradation mechanism, reducing the performance and lifetime of SOFC [2]. Furthermore, the strength of metal alloy heat exchanger decreases rapidly above temperature of 550 °C [3], thus the long-term operation under adverse conditions such as high temperature and oxidation will affect the dynamic service performance of alloy heat exchangers. SiC ceramics and their composite materials are considered as the most promising ceramic materials for high temperature heat exchangers due to their high intensity at high temperature, low density, low thermal expansion coefficient, high thermal conductivity, anti-oxidation, low creep at high temperature and excellent thermal shock resistance [4, 5], thus the application prospects of SiC in SOFC power generation system are promising.

For the high temperature nonmetal heat exchanger, relevant research in China has not been carried out yet, while the international research is just getting started. José Luis Córdova et al. [6, 7] designed and developed a novel cathode air preheater made of alumina ceramics for SOFC. The heat exchanger comprised a group of overlapping quasi-spiral flow channels with rectangular cross section, which was tested to achieve high heat transfer efficiency of 92% and low pressure drop. M. Dev Anand [8] and Umayorupagam P. et al. [9] compared the performance of compact heat exchangers with rectangular channels using SiC and AlN materials. Moreover, researchers have also investigated the application of SiC based high temperature heat exchangers in other fields [10–12]. The research on heat transfer and flow process is relatively simple, and the effect of heat radiation is also ignored in order to simplify heat transfer calculation. However, the temperature of flue gas in SOFC cathode air preheater can be as high as 1100 °C, and the flue gas side contain polar molecules such as CO_2 and H_2O, thus the flus gas has a certain radiation capacity. Furthermore, SiC ceramic heat transfer element has a dark color and rough surface, thus exhibits high blackness at high surface temperature, which can be approximately considered as blackbody. Therefore, the effect of thermal radiation may not be negligible.

To sum up, replacing the commonly used metal materials with high-temperature resistant SiC ceramic materials for the manufacturing of SOFC high-temperature heat exchanger is a revolutionary technology with great application potential. However, the research on coupled radiation-conduction-convection heat transfer characteristics of SiC high temperature heat exchanger in SOFC needs to be carried out urgently. This paper focused on SiC-based cathodic air preheater which is a novel SOFC high temperature heat exchanger. Based on ANSYS Fluent, the coupled heat transfer characteristics between flue gas and air at extremely high temperature conditions were firstly investigated and the effect of radiation heat transfer were analyzed.

2 Structure and Operating Parameters of SOFC Air Preheater

SOFC cathode air preheater comprises a series of high-temperature flue gas channels and air channels. In order to study the coupled radiation-conduction-convection heat transfer characteristics between flus gas and air, the heat exchanger is simplified as a tubular heat exchanger composed of a hot channel and a cold channel. Figure 1 shows the structure and operating conditions of tubular heat exchanger simulated in this paper. Table 1 shows the simulation parameters of the structure and operating conditions of a natural gas SOFC air preheater. The hydraulic diameter of the internal air channel is 5–10 mm, the internal diameter of the external flue gas channel is 10–20 mm, and the length along the channel is within 500 mm. The heat exchanger material is SiC. The flue gas inlet temperature is in the range of 800–1100 °C, with pressure of 1 bar and flow rate of 1–5 m/s. The flue gas components are H_2O (20–30%), CO_2 (10–20%), O_2 (0–10%) and N_2. The inlet air temperature is 25 °C, with pressure of 1 bar and flow rate of 1–5 m/s. The outlet air temperature is required no less than 700 °C.

(a) Structure of heat exchanger

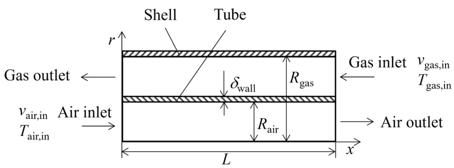

(b) Two-dimensional axisymmetric operation conditions

Fig. 1. Structure and operating conditions of simulated heat exchanger

3 Numerical Model

3.1 Radiative Transfer Equation

Considering the effect of heat radiation, the radiation heat flux must be introduced into the energy equation. In order to calculate the radiation heat flux, the Radiative Transfer Equation (RTE) must be introduced, and the temperature field should be solved by coupling the energy equation and RTE.

The RTE for radiation participating medium at position $\vec{r}$, in the direction $\vec{s}$ is as follows:

$$\frac{dI(\vec{r},\vec{s})}{ds} + (\alpha + \sigma_s)I(\vec{r},\vec{s}) = \alpha n^2 \frac{\sigma T^4}{\pi} + \frac{\sigma_s}{4\pi}\int_0^{4\pi} I(\vec{r},\vec{s}')\Phi(\vec{s},\vec{s}')d\Omega' \tag{1}$$

where, $\vec{s}$ is the position vector. $\vec{r}$ is the direction vector. $\vec{s}'$ is the scattering direction vector. s is the path length. α is the absorption coefficient. n is the refractive index. σ_s is the scattering coefficient. σ is the Stefan-Boltzmann constant. I is the radiation intensity. T is the local temperature. Φ is the phase function. Ω' is the solid angle.

Table 1. Simulation parameters of the structure and operating conditions.

Parameter		Value
Inlet gas temperature		800–1100 °C
Inlet gas velocity		1–5 m/s
Inlet gas pressure		1–2 bar
Gas components	N_2	40–70%
	H_2O	20–30%
	CO_2	10–20%
	O_2	0–10%
Inlet air temperature		25 °C
Inlet air velocity		1–5 m/s
Inlet air pressure		1–2 bar
Inner diameter of air channel		5–10 mm
Inner diameter of gas channel		10–20 mm
Thickness of channel		1–3 mm
Channel length		400–500 mm

3.2 Optical Thickness

Optical thickness (τ_λ) represents the heat radiation attenuation ability of radiation participating gas at a specific wavelength along given path length. High optical thickness value corresponds to high attenuation effect of the radiation participating gas on the incident radiation energy. τ_λ is the line integral of the attenuation coefficient along any path in a scattering and absorbing medium which can be expressed as follows:

$$\tau_\lambda = \int_0^L \kappa_\lambda(l)\mathrm{d}l \tag{2}$$

where, κ_λ is the spectral attenuation coefficient which depends on the gas components, pressure, temperature and the wavelength of incident radiation energy. κ_λ is the sum of the spectral absorption coefficient (α_λ) and spectral scattering coefficient ($\sigma_{s,\lambda}$) at a specific wavelength:

$$\kappa_\lambda = \alpha_\lambda + \sigma_{s,\lambda} \tag{3}$$

For uniform medium, spectral attenuation coefficient is constant along the path length L, thus optical thickness has a simple physical interpretation as the length of a path in units of mean free path which can be expressed as follows:

$$\tau_\lambda = \kappa_\lambda L \tag{4}$$

In this simulation, the diameter of flue gas channel is in the range of 5–10 mm, and the flue gas contains two polar molecules, CO_2 and H_2O. The absorption coefficient of CO_2 is about 0.5 m^{-1}, and the concentration of CO_2 is in the range of 10–20%. The absorption coefficient of H_2O is about 0.4 m^{-1}, and the concentration of H_2O is in the range of 20–30%. Thus, the optical thickness of flue gas is less than 0.005, which belongs to optical thin gas. In engineering estimation, the absorption effect of CO_2 and H_2O on incident radiation energy cannot be ignored, but their scattering effect can be ignored. Therefore, to preliminarily analyze the effect of flue gas radiation on heat exchanger performance, the pure absorption and non-scattering condition of gray gas is simulated in this study.

3.3 Radiation Heat Transfer Model

In this paper, DO model was selected to simulate the radiation heat transfer between high-temperature flue gas and air. In addition, S2S model calculation results can be used as comparison to analyze the effect of gas radiation.

(1) **DO model**

DO model is applicable to radiation problems in entire range of optical thicknesses. It allows the solution of enclosure radiative transfer without participating media and participating radiation. The DO model solves the RTE of a finite number of discrete solid angles, and the solution precision is controlled by the precision of the discrete solid angles. DO model considers the RTE in the position $\vec{s}$ as a field equation as follows:

$$\nabla(I(\vec{r},\vec{s})\vec{s}) + (\alpha + \sigma_s)I(\vec{r},\vec{s}) = \alpha n^2 \frac{\sigma T^4}{\pi} + \frac{\sigma_s}{4\pi}\int_0^{4\pi} I(\vec{r},\vec{s}')\Phi(\vec{s},\vec{s}')d\Omega' \tag{5}$$

(2) **S2S model**

The S2S model is suitable for the solution of enclosure radiative transfer without participating media, however it assumes that all surfaces are diffuse and gray radiation. Thus, S2S model cannot be used to model participating radiation problems. The emissivity (ε) equals the absorptivity (α) and the transmissivity could be neglected. When radiant energy (E) is incident on the surface, part (ρE) is reflected, part (αE) is absorbed, and part (τE) is transmitted. Considering the conservation of energy, that $\alpha + \rho = 1$. Since $\alpha = \varepsilon$, thus $\rho = 1 - \varepsilon$.

The radiation heat flux leaving a given surface consists of directly emitted heat flux and reflected heat flux. The reflected heat flux depends on the incident heat flux from the surroundings, which can be expressed by the radiant heat flux leaving all other surfaces. The radiation heat flux leaving from surface k can be expressed as follows:

$$q_{\text{out},k} = \varepsilon_k \sigma T^4 + \rho_k q_{\text{in},k} \tag{6}$$

where, $q_{\text{out},k}$ is the radiation heat flux leaving the surface. ε_k is the emissivity. ρ_k is the reflectivity. $q_{\text{in},k}$ is the radiation heat flux incident on the surface from the surroundings.

The radiant heat flux incident from one surface to another can be calculated by the surface to-surface view factor (F_{jk}). Therefore, incident radiant heat flux can be expressed as radiant heat flux leaving all other surfaces as:

$$q_{in,k} = \sum_{j=1}^{N} F_{kj} q_{out,j} \tag{7}$$

Then, the total radiant heat flux leaving surface k can be rewritten as:

$$q_{out,k} = \varepsilon_k \sigma T^4 + \rho_k \sum_{j=1}^{N} F_{kj} q_{out,j} \tag{8}$$

Equation (8) can be written as follows:

$$J_k = E_k + \rho_k \sum_{j=1}^{N} F_{kj} J_j \tag{9}$$

where, J_k represents the heat flux given off from surface k, and E_k represents the emissive heat flux of surface k.

3.4 Grid Independence Study

A two-dimensional axisymmetric model of coupled radiation-conduction-convection heat transfer between flue gas and water was built according Fig. 1a. The flue gas domain, air domain and channel domain were divided into grids as shown in Fig. 2. The RTE and energy equations are solved based on ANSYS Fluent. A grid independence study was conducted to assess the appropriate number of grid elements. Different grid elements of 2×10^3, 5×10^3, and 1×10^4 were evaluated. Figure 3 showed the comparison of air temperature variation along the channel length calculated with different grid elements. It is found that grid elements of 5×10^3 is adequate for the simulation.

Fig. 2. Meshing of simulated heat exchanger

4 Results and Discussion

4.1 Radiation Model Comparison

In this section, DO model and S2S model in ANSYS Fluent were utilized to analyze the coupled radiation-conduction-convection heat transfer characteristics between high-temperature flue gas and air, and the simulation results were compared with the non-radiation model to analyze the effect of radiation. The detailed simulation parameters were listed in Table 2.

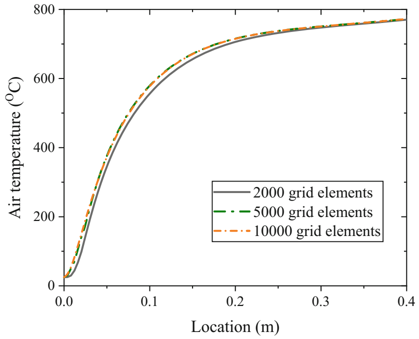

Fig. 3. Air temperature variation at different grid elements

Table 2. Simulation parameters of different cases.

Parameter		Case 1	Case 2	Case 3
Inlet gas temperature		800 °C		
Inlet gas velocity		3 m/s		
Inlet gas pressure		1 bar		
Gas components	N_2	40%		
	H_2O	30%		
	CO_2	20%		
	O_2	10%		
Inlet air temperature		25 °C		
Inlet air velocity		3 m/s		
Inlet air pressure		1 bar		
Inner diameter of air channel		5 mm	10 mm	10 mm
Inner diameter of gas channel		15 mm	20 mm	15 mm
Thickness of channel		1 mm		
Channel length		400 mm		

Figure 4 showed the temperature distributions of coupled heat transfer calculated by the DO radiation model, S2S radiation model and non-radiation model at case 1. It was found that the air outlet temperature was low without considering the radiation while the air outlet temperature is high considering the radiation. This means that the effect of radiation heat transfer cannot be ignored at high flue gas inlet temperature. Comparing the results of different radiation models, it can be seen that the calculation results of DO radiation model and S2S radiation model are very close. Thus, it was preliminarily considered that the effect of gas radiation on coupled heat transfer is tiny, and the effect of gas radiation can be ignored in the coupled heat transfer process, which indicates that the gray gas hypothesis is reasonable.

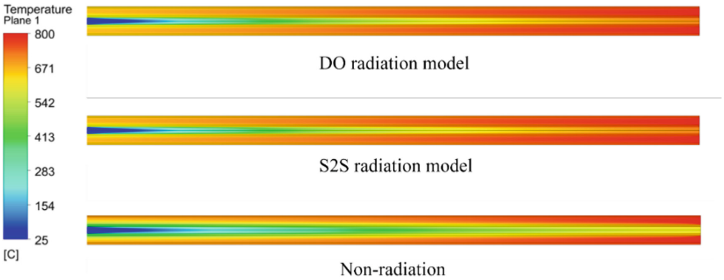

Fig. 4. Comparison of temperature distribution of different radiation models at case 1

Figures 5 and 6 showed the temperature variations of flue gas and air calculated by the DO radiation model, S2S radiation model and non-radiation model at case 1. It was found that the air temperature along the channel increases slightly when considering the radiation. When the flue gas inlet temperature is 800 °C, the air outlet temperature can only be heated to 600 °C. The air temperature along the channel increases greatly when considering the radiation, and the air outlet temperature can be heated to 700 °C. With high flue gas inlet temperature, the contribution of radiation heat transfer to air heating can be as high as 100 °C, thus the influence of radiation heat transfer is very important. Comparing the results of different radiation models, it can be seen that the calculation results of DO radiation model and S2S radiation model are very close, so the influence of gas radiation on heat transfer can be ignored at case 1.

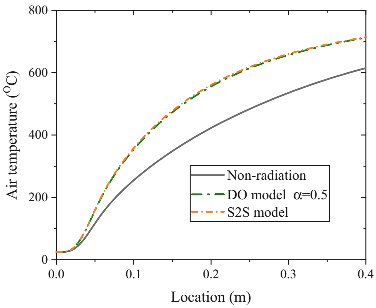

Fig. 5. Air temperature variation at case 1

Figures 7 and 8 showed the temperature variations of flue gas and air calculated by the DO radiation model, S2S radiation model and non-radiation model at case 2. The diameter of air channel in case 2 is larger than that in case 1, thus the ratio of air flow rate to flue gas flow rate in case 2 is larger than that in case 1 under the same inlet velocity, which leads to lower air outlet temperature in case 2. Regardless of radiation heat transfer, the air outlet temperature can only be heated to 320 °C. Considering the radiation heat transfer, the air outlet temperature calculated by S2S radiation model is 420 °C, and air outlet temperature calculated by DO radiation model is 400 °C. On one hand, the contribution of radiation heat transfer to air heating at case 2 is up to 100 °C,

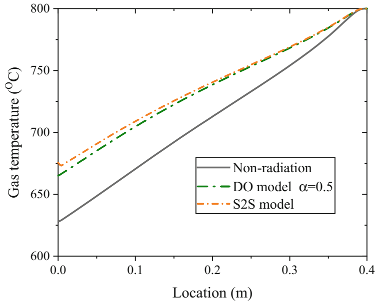

Fig. 6. Flue gas temperature variation at case 1.

which further proves the importance of radiation heat transfer to coupled heat transfer. On the other hand, comparing the results of different radiation models, it is found that there is a deviation between the DO radiation model and the S2S radiation model results, that is, the gas radiation will affect the proportion of radiation heat transfer at case 2, which indicates that the gas radiation has a certain effect on the coupled heat transfer when the air/gas flow ratio is large. In addition, the air outlet temperature calculated by the S2S radiation model is higher than that calculated by the DO radiation model, which indicates the existence of radiation participating gases slightly reduce the coupled heat transfer characteristics.

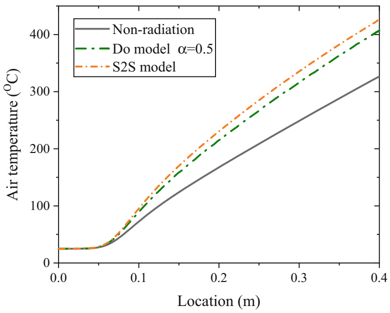

Fig. 7. Air temperature variation at case 2

Figures 9 and 10 showed the temperature variations of flue gas and air calculated by the DO radiation model, S2S radiation model and non-radiation model at case 3. The diameter of flue gas channel in case 3 is smaller than that in case 2, thus the ratio of air flow rate to flue gas flow rate in case 3 is larger than that in case 1 and case 2 under the same inlet velocity, which leads to lower air outlet temperature in case 3. The air outlet temperature can only be heated to 250 °C without considering radiation heat transfer. Considering the radiation heat radiation heat transfer, air outlet temperature calculated by the S2S radiation model is 290 °C and the DO radiation is 270 °C. On one hand, the contribution of radiation heat transfer to air heating is 20–40 °C in case 3, which means the effect of radiation heat transfer on coupled heat transfer is reduced in case 3. On the

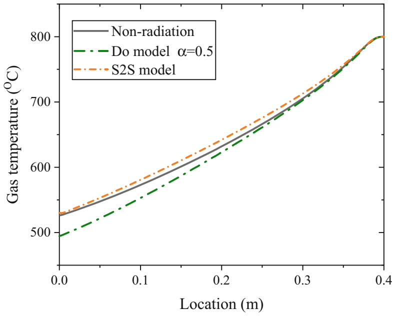

Fig. 8. Flue gas temperature variation at case 2.

other hand, comparing the results of different radiation models, it can be seen that the air outlet temperature calculated by S2S radiation model is higher than that calculated by DO radiation model, which further proves that gas radiation has certain effect on the coupled heat transfer when the air/gas flow ratio is large.

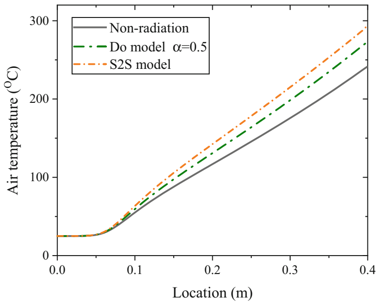

Fig. 9. Air temperature variation at case 3.

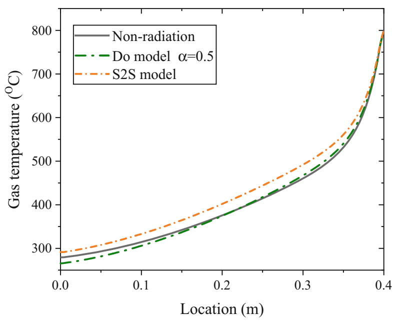

Fig. 10. Flue gas temperature variation at case 3.

4.2 Effect of Absorption Coefficient

According to above analysis, the gas radiation has a certain impact on the coupled heat transfer characteristics only at large air/gas flow ratio. Since the SOFC cathode air preheater in this study is designed to heat the air to above 700 °C using high-temperature flue gas, the air/ gas flow ratio is generally small, thus the effect of gas radiation is unapparent. In addition, the optical thickness of flue gas is very tiny (less than 0.005), thus the gas radiation effect is very tiny. Based on the above analysis, the flue gas radiation has little effect on the coupled heat transfer characteristics.

To further verify the effect of flue gas radiation on the coupled heat transfer characteristics, the gray gas assumption is adopted in this section considering the flue gas absorption coefficient to be independent of wavelength, thus the average absorption coefficient is used in calculation. The DO radiation model is used to analyze the effect of the absorption coefficient on the coupled heat transfer characteristics of flue gas and air with the flue gas absorption coefficient in the range of 0–1 m^{-1}. Figures 11, 12 and 13 showed the air and flue gas temperature variations along the channel with different absorption coefficients at case 1–3. It is found that the absorption coefficient of flue gas in the DO radiation model has little effect on the air and flue gas temperature variation with inlet flue gas temperature of 800 °C at each case. Thus, when inlet flue gas temperature is not very high, the effect of gas radiation can be ignored.

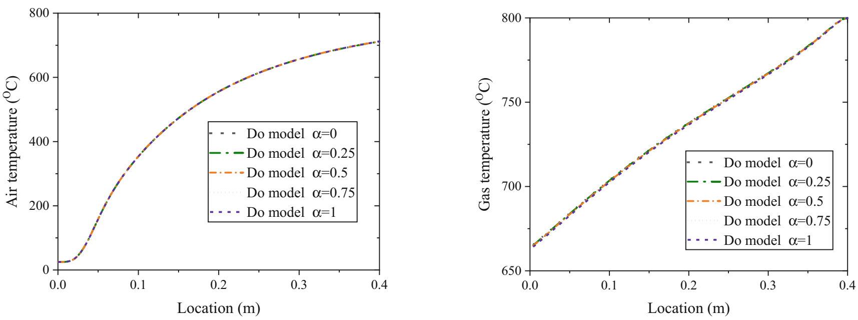

Fig. 11. Air and flue gas temperature variation along the channel at case 1 with different absorption coefficients.

Figures 14 and 15 showed the effect of absorption coefficient on air and flue gas temperature variation at case 2 with inlet flue gas temperature of 1100 °C and 1500 °C, respectively. It is found that the absorption coefficient of flue gas has little effect on the air temperature variation with high inlet flue gas temperature, while has small effect on the flue gas temperature variation. Moreover, the higher the inlet flue gas temperature, the greater the effect on the flue gas temperature variation. Since the flue gas temperature in the SOFC cathode air preheater is in the range of 800–1100 °C, the effect of flue gas absorption coefficient and gas radiation can be ignored.

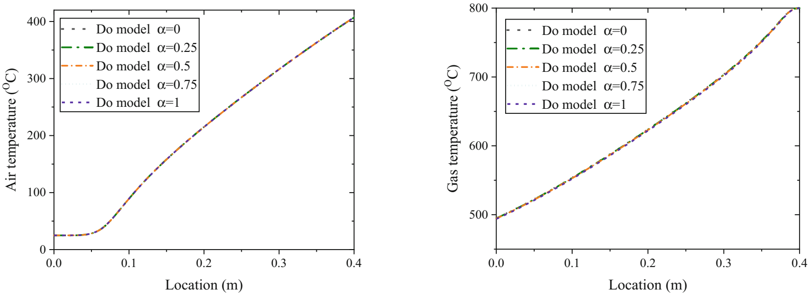

Fig. 12. Air and flue gas temperature variation along the channel at case 2 with different absorption coefficients.

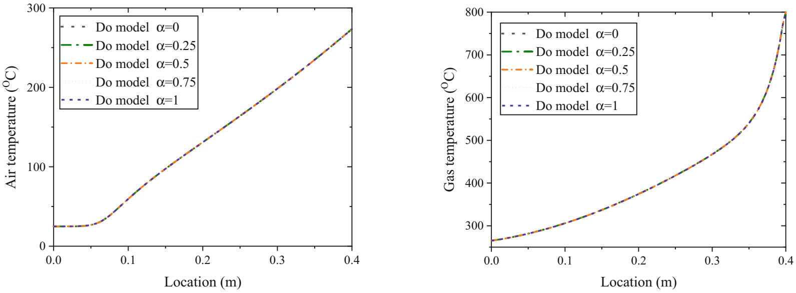

Fig. 13. Air and flue gas temperature variation along the channel at case 3 with different absorption coefficients

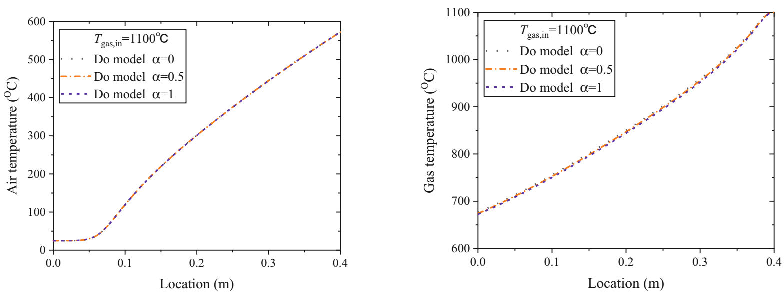

Fig. 14. Effect of absorption coefficient on flue gas temperature variation at inlet flue gas temperature of 1100 °C.

5 Conclusions

(1) The air outlet temperature calculated by the non-radiation model is apparently lower than that of DO radiation model and S2S radiation model, thus the effect of radiation heat transfer is very important and cannot be ignored at high flue gas inlet temperature.

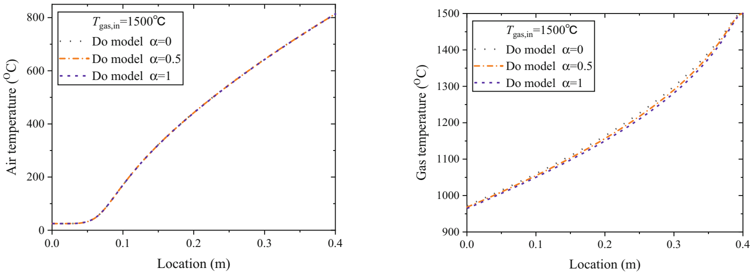

Fig. 15. Effect of absorption coefficient on flue gas temperature variation at inlet flue gas temperature of 1500 °C.

(2) Comparing different radiation models, the calculation results of DO radiation model and S2S radiation model are very close at small air/gas flow rate ratio, while the calculation results of S2S radiation model is slightly higher than DO radiation model at large air/gas flow rate ratio. Thus, the participating radiation effect of flue gas slightly deteriorates the coupled heat transfer characteristics.

(3) The absorption coefficient of flue gas has little effect on the air temperature variation, while has tiny effect on flue gas temperature variation at high flue gas inlet temperature of 1100–1500 °C. The higher the flue gas inlet temperature, the greater the effect on the flue gas temperature variation.

Acknowledgements. This research is sponsored by the Doctor's Science and Technology Fund of HGMRI (2020011749) and Youth's science and technology Fund of SINOMACH (QNJJ-ZD-2022-06).

References

1. Hu, L., Yang, Z.B., Xiong, X.Y., et al.: Development strategy for solid oxide fuel cell industry in China. Strateg. Study Chin. Acad. Eng. **24**(3), 118–126 (2022)
2. Giles, S., Lin, G., Mohanram, A., et al.: Saint-Gobain's all ceramic SOFC stack: architecture and performance. ECS Trans. **57**(1), 105–114 (2013)
3. Caccia, M., Tabandeh-Khorshid, M., Itskos, G., et al.: Ceramic–metal composites for heat exchangers in concentrated solar power plants. Nature **562**(7727), 346–347 (2018)
4. Sommers, A., Wang, Q., Han, X., et al.: Ceramics and ceramic matrix composites for heat exchangers in advanced thermal systems—a review. Appl. Therm. Eng. **30**(11–12), 1277–1291 (2010)
5. Li, Q., et al.: Compact heat exchangers: a review and future applications for a new generation of high temperature solar receivers. Renew. Sustain. Energy Rev. (2011)
6. Cordova, J.L.: Novel compact ceramic heat exchanger for solid oxide fuel cell cathode air preheater application. In *16th Annual Solid Oxide Fuel Cell Workshop* (2015)
7. Córdova, J.L., Heshmat, H.: Development of a ceramic heat exchanger for application as solid oxide fuel cell cathode air preheater. In *ASME Power & Energy Conference* (2016)

8. Anand, M.D., Devadhas, G.G., Prabhu, N., et al.: ceramic monolith heat exchanger—a theoretical study and performance analysis (2018)
9. Arunachalam, U.P., Edwin, M.: Theoretical investigation of a ceramic monolith heat exchanger using silicon carbide and aluminium nitride as heat exchanger material. Int. J. Heat Technol. **35**(3), 645–650 (2017)
10. Schulte-Fischedick, J., DreißIgacker, V., Tamme, R.: An innovative ceramic high temperature plate-fin heat exchanger for EFCC processes. Appl. Therm. Eng. **27**(8–9), 1285–1294 (2007)
11. Nagarajan, V., Chen, Y., Wang, Q., et al.: Hydraulic and thermal performances of a novel configuration of high temperature ceramic plate-fin heat exchanger. Appl. Energy **113**(Jan.), 589–602 (2014)
12. Takeuchi, Y., Park, C., Noborio, K., et al.: Heat transfer in SiC compact heat exchanger. Fusion Eng. Des. **85**(7–9), 1266–1270 (2010)